Power Saving Design of Active Reconfigurable Intelligent Surface—A Sub-Array Architecture

Yanze Zhu[1], Yang Liu[1*], Ming Li[1], Qingqing Wu[2], and Qingjiang Shi[3]
1: School of Information and Communication Engineering, Dalian University of Technology
2: Department of Electrical and Computer Engineering, University of Macau
3: School of Software Engineering, Tongji University, and Shenzhen Research Institute of Big Data
Emails: {5476z4969y5283z@mail.dlut.edu.cn, yangliu_613@dlut.edu.cn, mli@dlut.edu.cn, qingqingwu@um.edu.mo, shiqj@tongji.edu.cn}

***Abstract*—Reconfigurable intelligent surface (RIS) is envisioned as a promising technology to enhance future wireless communication systems. Very recently, a novel *active* RIS architecture has been proposed via introducing amplifiers into the reflecting elements. Although these embedded amplifiers can effectively extend the RIS coverage, they also bring non-negligible energy expenditure. To overcome this drawback, this paper proposes a novel sub-array based structure, which divides the entire RIS array into multiple sub-arrays with each being flexibly turned on/off. We aim to minimize the power consumption of the whole system via jointly activating sub-arrays and designing beamforming, which is highly challenging due to its combinatorial nature. Via inducing the group sparsity and leveraging the majorization-minimization (MM) approach, we develop an efficient solution to resolve this challenge. Numerical results demonstrate that our proposed sub-array structure can significantly reduce the power consumption compared to the conventional "all-on" scheme.**

***Index Terms*—Active reconfigurable intelligent surface (RIS), power minimization, group sparsity, beamforming.**

I. Introduction

A. Background

The emerging reconfigurable intelligent surface (RIS) [1], which is also widely known as intelligent reflecting surface (IRS) [2], has been cast with great attentions due to its capability in improving wireless communication performances in many aspects, including reducing transmit radio power (TRP) of the access point (AP) [3], enhancing cell-edge coverage [4], improving energy efficiency (EE) [5] and so on. In spite of the aforementioned advantages, some recent researches have uncovered that the passive RIS suffers from severe "double fading" effect [6], [7]. This means the fading attenuation associated with the cascaded channel by way of the RIS is much more severe (generally several orders of multitude) than that of the direct channel. Double fading phenomenon dramatically restricts the coverage of the passive RIS.

To combat the double fading effect, a novel active RIS architecture has been proposed very recently [7]. Compared to the traditional passive RIS, the active RIS utilizes amplifiers in each "reflecting" element to magnify the incident signals. A number of recent works have manifested the advantages of active RIS over its passive counterpart in improving signal-to-noise-ratio (SNR) [7]-[9], enhancing secure communication [10], maximizing network throughput [11] and so on.

* Corresponding author.

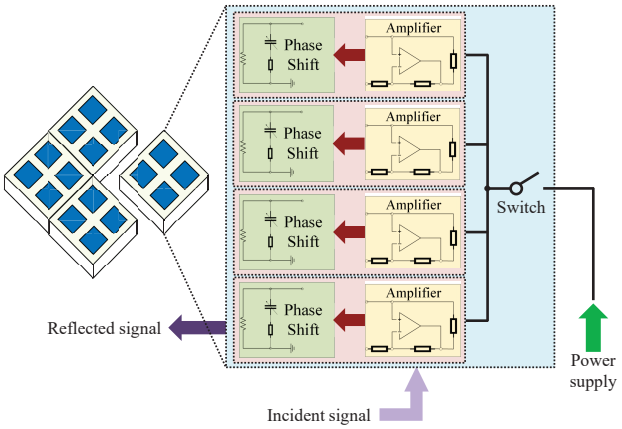

Fig. 1. Proposed sub-array based active RIS structure.

Although the newly proposed active RIS architecture has been demonstrated to be capable of effectively overcoming the double fading effect, the introduced amplifiers also boosts the energy expenditure of the RIS at the same time. This issue has not yet been extensively investigated by any existing literature. In this paper, based on the active RIS architecture [7], we propose a more flexible structure in order to reduce the power consumption of the RIS device.

B. Motivation

Before elaborating our proposal, we firstly review the power consumption of the active RIS device. As pointed out by [12], the energy expenditure of wireless communication devices mainly comes from non-transmit power consumption. As for the active RIS, the energy consumed by the phase shifter and amplifier takes up the most proportion of power consumption of each active RIS element. According to the existing literature [9], [13], the non-transmit power of an active RIS element generally takes a value from 2mW to 10mW for realistic implementation. Consider the RIS device with 300 reflecting elements, each of which has a power consumption of 5mW. Then, its total power consumption can reach up to 1.5W when

all elements are working, which is comparable to that of a femto-cell AP (at a level of several Watts [12], [14]). For instance, the Huawei device AP1050DN-S has an average power consumption of 5W [14]. The above observations motivate us to appropriately switch off a fraction of active RIS elements to save power. On the one hand, more working RIS elements can provide larger beamforming gain. On the other hand, however, more activated RIS elements will consume more non-transmit power due to the phase shifters and amplifiers. Intuitively, we need to select and activate the RIS elements with advantageous fading gains while shutting off the others. Towards this end, we propose a sub-array based architecture, where each sub-array is controlled by a switch and can be switched on/off on demand, as shown in Fig. 1.

II. System Model and Problem Formulation

A. System Model

Consider a downlink system where an AP equipped with M_{AP} antennas serves K single-antenna users. An active RIS with N_{RIS} reflecting elements is deployed to assist this system, as illustrated in Fig. 2. The sets of users and reflecting elements are denoted by $\mathcal{K} \triangleq \{1, \cdots, K\}$ and $\mathcal{N} \triangleq \{1, \cdots, N_{\mathrm{RIS}}\}$, respectively.

Suppose that we group these elements into M_{RIS} sub-arrays, each of which consists of L_{RIS} reflecting elements. Hence, the total number of reflecting elements N_{RIS} is calculated by $N_{\mathrm{RIS}} = M_{\mathrm{RIS}} L_{\mathrm{RIS}}$. The set of sub-arrays is defined by $\mathcal{M} \triangleq \{1, \cdots, M_{\mathrm{RIS}}\}$. The reflecting coefficient vector of the mth sub-array can be expressed as $\boldsymbol{\theta}_m \triangleq [\beta_{(m-1)L_{\mathrm{RIS}}+1} e^{j\theta_{(m-1)L_{\mathrm{RIS}}+1}}, \cdots, \beta_{mL_{\mathrm{RIS}}} e^{j\theta_{mL_{\mathrm{RIS}}}}]^T,\ m \in \mathcal{M}$, where $\beta_n,\ n \in \mathcal{N}$, represents the amplifier coefficient and $\theta_n \in [0, 2\pi),\ n \in \mathcal{N}$, stands for the phase shift of the nth reflecting element. Meanwhile, we have $\beta_n \in (0, \beta_{n,\max}],\ n \in \mathcal{N}$, with $\beta_{n,\max},\ n \in \mathcal{N}$, denoting the maximal magnifying factor of the nth amplifier due to the limited magnifying capability of amplifiers. Moreover, the reflecting coefficient matrix of the RIS is defined by $\boldsymbol{\Theta} \triangleq \mathrm{blkdiag}\{\boldsymbol{\Theta}_1, \cdots . \boldsymbol{\Theta}_{M_{\mathrm{RIS}}}\}$, where $\boldsymbol{\Theta}_m \triangleq \mathrm{diag}(\boldsymbol{\theta}_m),\ m \in \mathcal{M}$. Besides, the set of activated sub-arrays is denoted by $\mathcal{A} \subseteq \mathcal{M}$. If $i \in \mathcal{A}$, then the ith sub-array is turned on, i.e, $\boldsymbol{\Theta}_i \neq \mathbf{O}_{L_{\mathrm{RIS}}}$, otherwise, $\boldsymbol{\Theta}_i = \mathbf{O}_{L_{\mathrm{RIS}}}$ with $\mathbf{O}_{L_{\mathrm{RIS}}}$ indicating an all-zero $L_{\mathrm{RIS}} \times L_{\mathrm{RIS}}$ matrix. It is worth noting that our aforementioned model will boil down to an element-wise activation scheme when each sub-array only comprises one reflecting element, i.e., $L_{\mathrm{RIS}} = 1$.

The AP transmits the signal which reads as

$$\boldsymbol{x}_{\mathrm{AP}} = \sum\nolimits_{k=1}^{K} \boldsymbol{f}_k s_k, \tag{1}$$

where $s_k \in \mathbb{C},\ k \in \mathcal{K}$, represents the symbol transmitted to the kth user and $\boldsymbol{f}_k \in \mathbb{C}^{M_{\mathrm{AP}}},\ k \in \mathcal{K}$, stands for the associated beamformer. Without loss of generality, suppose $\mathbb{E}\{s_k\} = 0$, $\mathbb{E}\{|s_k|^2\} = 1,\ k \in \mathcal{K}$. Besides, it is reasonable to assume that different s_k's are mutually uncorrelated.

Define $\mathbf{G} \in \mathbb{C}^{M_{\mathrm{AP}} \times N_{\mathrm{RIS}}}$, $\boldsymbol{h}_{\mathrm{d},k}^H \in \mathbb{C}^{1 \times M_{\mathrm{AP}}},\ k \in \mathcal{K}$, and $\boldsymbol{h}_{\mathrm{r},k}^H \in \mathbb{C}^{1 \times N_{\mathrm{RIS}}},\ k \in \mathcal{K}$, as the channels from the AP to the RIS, from the AP to the kth user and from the RIS to the kth user, respectively. Then, the RIS receives the signal from the AP which can be expressed as

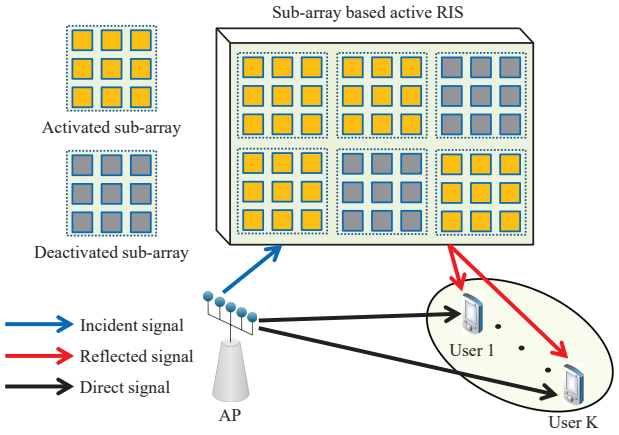

Fig. 2. An active RIS aided MU-MISO system based on sub-array.

$$\boldsymbol{y}_{\mathrm{RIS}} = \mathbf{G}\boldsymbol{x}_{\mathrm{AP}} + \boldsymbol{n}_{\mathrm{RIS}}, \tag{2}$$

where $\boldsymbol{n}_{\mathrm{RIS}} \in \mathbb{C}^{N_{\mathrm{RIS}}}$ denotes the thermal noise at the RIS with $\boldsymbol{n}_{\mathrm{RIS}} \sim (\mathbf{0}, \sigma_{\mathrm{RIS}}^2 \mathbf{I}_N)$ and $\mathbf{I}_N$ indicates an $N \times N$ identity matrix.

After reflected and amplified via the RIS, the incoming signal will be adjusted as

$$\boldsymbol{x}_{\mathrm{RIS}} = \boldsymbol{\Theta}\boldsymbol{y}_{\mathrm{RIS}} = \boldsymbol{\Theta}(\mathbf{G}\boldsymbol{x}_{\mathrm{AP}} + \boldsymbol{n}_{\mathrm{RIS}}). \tag{3}$$

The signals from the AP and the RIS combine at the kth user, which can be given by

$$y_k = \boldsymbol{h}_{\mathrm{r},k}^H \boldsymbol{x}_{\mathrm{RIS}} + \boldsymbol{h}_{\mathrm{d},k}^H \boldsymbol{x}_{\mathrm{AP}} + n_k,\ k \in \mathcal{K}, \tag{4}$$

where $n_k \in \mathbb{C},\ k \in \mathcal{K}$, is the thermal noise at the kth user. For simplicity, it is supposed that $n_k \sim (0, \sigma_k^2),\ k \in \mathcal{K}$, and each n_k is uncorrelated with other $n_j,\ k, j \in \mathcal{K},\ j \neq k$.

The signal-to-interference-plus-noise-ratio (SINR) can be calculated from (4) as

$$\mathsf{SINR}_k(\mathbf{F}, \boldsymbol{\Theta}) = \frac{|\boldsymbol{h}_k^H \boldsymbol{f}_k|^2}{\sum_{j=1, j\neq k}^{K} |\boldsymbol{h}_k^H \boldsymbol{f}_j|^2 + \sigma_{\mathrm{RIS}}^2 \|\boldsymbol{\Theta}^H \boldsymbol{h}_{\mathrm{r},k}\|_2^2 + \sigma_k^2},\ k \in \mathcal{K}, \tag{5}$$

where $\mathbf{F} \triangleq \{\boldsymbol{f}_k\}_{k=1}^K$ and $\boldsymbol{h}_k^H \triangleq \boldsymbol{h}_{\mathrm{r},k}^H \boldsymbol{\Theta} \mathbf{G} + \boldsymbol{h}_{\mathrm{d},k}^H,\ k \in \mathcal{K}$, represents the equivalent channel between the AP and the kth user. Then, the achievable rate of the system is

$$\mathsf{R}_{\mathrm{total}}(\mathbf{F}, \boldsymbol{\Theta}) = \sum\nolimits_{k=1}^{K} \log(1 + \mathsf{SINR}_k(\mathbf{F}, \boldsymbol{\Theta})). \tag{6}$$

Besides, based on the previous discussion, if the ith sub-array is switched off, $\boldsymbol{\theta}_i$ will be a zero vector. Therefore, by denoting $\tilde{\boldsymbol{\theta}} \triangleq [\|\boldsymbol{\theta}_1\|_2, \cdots, \|\boldsymbol{\theta}_{M_{\mathrm{RIS}}}\|_2]^T$, the cardinality of $\mathcal{A}$ can be equivalently written as

$$|\mathcal{A}| = \|\tilde{\boldsymbol{\theta}}\|_0, \tag{7}$$

where the ℓ_0-norm counts the number of the non-zero elements of the input vector.

B. Power Consumption Model

Here we discuss the power consumption model including sub-array activation of the whole system.

Firstly, the power consumption at the AP is given by

$$\mathsf{P}_{\mathrm{AP}}(\mathbf{F}) = \xi_{\mathrm{AP}} \sum\nolimits_{k=1}^{K} \|\boldsymbol{f}_k\|_2^2 + P_{\mathrm{c,AP}}, \tag{8}$$

where ξ_{AP} represents the inverse of the emission efficiency of the AP, $P_{\mathrm{c,AP}}$ stands for the energy consumed by signal processing and local hardware at the AP.

Secondly, the power consumption at the RIS reads as

$$\begin{aligned}\mathsf{P}_{\mathrm{RIS}}(\mathbf{F}, \boldsymbol{\Theta}) = \xi_{\mathrm{RIS}} \left(\sum\nolimits_{k=1}^{K} \|\boldsymbol{\Theta}\mathbf{G}\boldsymbol{f}_k\|_2^2 + \sigma_{\mathrm{RIS}}^2 \|\boldsymbol{\Theta}\|_F^2 \right) \\ + \|\tilde{\boldsymbol{\theta}}\|_0 L_{\mathrm{RIS}}(P_{\mathrm{PS}} + P_{\mathrm{A}}),\end{aligned} \tag{9}$$

where ξ_{RIS} indicates the inverse of the emission efficiency of the RIS amplifiers, P_{PS} and P_{A} represent the dissipated power of the phase shifter and the amplifier, respectively. In general, $P_{\mathrm{c,RIS}} \triangleq P_{\mathrm{PS}} + P_{\mathrm{A}}$ is regarded as a constant [9], [13].

Lastly, the power consumed by all users can be expressed as

$$P_{\mathrm{user}} = \sum\nolimits_{k=1}^{K} P_{\mathrm{c},k}, \tag{10}$$

where $P_{\mathrm{c},k},\ k \in \mathcal{K}$, stands for the dissipated power at the kth user, which is generally viewed as a constant for downlink scenarios [5], [13].

To sum up, the total power consumption of the considered system is given as follows

$$\mathsf{P}_{\mathrm{total}}(\mathbf{F}, \boldsymbol{\Theta}) = \mathsf{P}_{\mathrm{AP}}(\mathbf{F}) + \mathsf{P}_{\mathrm{RIS}}(\mathbf{F}, \boldsymbol{\Theta}) + P_{\mathrm{user}}. \tag{11}$$

C. Problem Formulation

We aim to minimize $\mathsf{P}_{\mathrm{total}}(\mathbf{F}, \boldsymbol{\Theta})$ via jointly designing sub-array activation pattern and beamformings of the AP and the RIS while satisfying the quality-of-service (QoS) requirements for the users, which can be formulated as

$$(\mathcal{P}1):\ \min_{\mathbf{F}, \boldsymbol{\Theta}}\ \mathsf{P}_{\mathrm{total}}(\mathbf{F}, \boldsymbol{\Theta}) \tag{12}$$

$$\text{s.t.} \sum\nolimits_{k=1}^{K} \|\boldsymbol{f}_k\|_2^2 \le P_{\mathrm{AP,max}}, \tag{12a}$$

$$\mathsf{P}_{\mathrm{RIS}}(\mathbf{F}, \boldsymbol{\Theta}) \le P_{\mathrm{RIS,max}}, \tag{12b}$$

$$\log(1 + \mathsf{SINR}_k(\mathbf{F}, \boldsymbol{\Theta})) \ge R_k,\ k \in \mathcal{K}, \tag{12c}$$

$$\beta_n \le \beta_{n,\max},\ \theta_n \in [0, 2\pi),\ n \in \mathcal{N}, \tag{12d}$$

where $P_{\mathrm{AP,max}}$ in (12a) and $P_{\mathrm{RIS,max}}$ in (12b) represent the maximal power supply at the AP and the RIS, respectively, and (12c) describes the QoS thresholds for all users.

III. Proposed Algorithm

A. Approximation and Group Sparsity Inducing

Firstly, it can be observed that the main difficulty to solve $(\mathcal{P}1)$ comes from the non-convex and non-smooth term $\|\tilde{\boldsymbol{\theta}}\|_0$. Note that exhaustively searching all $(2^{M_{\mathrm{RIS}}} - 1)$ possible sub-array activation patterns can result in a near-optimal solution, however, this will also yield unrealistically high complexity.

We exploit smooth approximations to surrogate the ℓ_0-norm to deal with the non-smoothness of it. Actually, the authors in [15] have presented a bunch of well-behaved smooth functions to achieve this goal, including parameterized logarithm/exponential/arctangent functions, which can all be further tackled by the majorization-minimization (MM) methodology [16] and exhibit similar performance [15]. We will select the logarithm function to approximate ℓ_0-norm in the following. Particularly, the ℓ_0-norm can be smoothed by

$$\|\tilde{\boldsymbol{\theta}}\|_0 \approx \sum\nolimits_{m=1}^{M_{\mathrm{RIS}}} \frac{\log\left(\frac{\|\boldsymbol{\theta}_m\|_2}{\delta} + 1\right)}{\log\left(\frac{1}{\delta} + 1\right)}, \tag{13}$$

where the parameter δ is a predefined positive constant and controls the precision of approximation. To yield a satisfying approximation, $\delta \in [10^{-6}, 10^{-5}]$ is a typical setting.

Define $\tilde{\mathsf{P}}_{\mathrm{RIS}}(\mathbf{F}, \boldsymbol{\Theta})$ and $\tilde{\mathsf{P}}_{\mathrm{total}}(\mathbf{F}, \boldsymbol{\Theta})$ as the functions after substituting (13) into (9) and (11), respectively. In the following, we focus on solving the approximated problem as follows

$$(\mathcal{P}2):\ \min_{\mathbf{F}, \boldsymbol{\Theta}}\ \tilde{\mathsf{P}}_{\mathrm{total}}(\mathbf{F}, \boldsymbol{\Theta}) \tag{14}$$

$$\text{s.t.} \sum\nolimits_{k=1}^{K} \|\boldsymbol{f}_k\|_2^2 \le P_{\mathrm{AP,max}}, \tag{14a}$$

$$\tilde{\mathsf{P}}_{\mathrm{RIS}}(\mathbf{F}, \boldsymbol{\Theta}) \le P_{\mathrm{RIS,max}}, \tag{14b}$$

$$\log(1 + \mathsf{SINR}_k(\mathbf{F}, \boldsymbol{\Theta})) \ge R_k,\ k \in \mathcal{K}, \tag{14c}$$

$$\beta_n \le \beta_{n,\max},\ \theta_n \in [0, 2\pi),\ n \in \mathcal{N}. \tag{14d}$$

The intractable rate function in (15c) makes $(\mathcal{P}2)$ still difficult to tackle. Inspired by the weighted minimal mean square error (WMMSE) method [17], the above problem can be equivalently transformed as

$$(\mathcal{P}3):\ \min_{\mathbf{F}, \boldsymbol{\Theta}, \boldsymbol{w}, \boldsymbol{v}}\ \tilde{\mathsf{P}}_{\mathrm{total}}(\mathbf{F}, \boldsymbol{\Theta}) \tag{15}$$

$$\text{s.t.} \sum\nolimits_{k=1}^{K} \|\boldsymbol{f}_k\|_2^2 \le P_{\mathrm{AP,max}}, \tag{15a}$$

$$\tilde{\mathsf{P}}_{\mathrm{RIS}}(\mathbf{F}, \boldsymbol{\Theta}) \le P_{\mathrm{RIS,max}}, \tag{15b}$$

$$\tilde{\mathsf{R}}_k(\boldsymbol{v}, \boldsymbol{w}, \mathbf{F}, \boldsymbol{\Theta}) \ge R_k,\ k \in \mathcal{K}, \tag{15c}$$

$$\beta_n \le \beta_{n,\max},\ \theta_n \in [0, 2\pi),\ n \in \mathcal{N}, \tag{15d}$$

where $\tilde{\mathsf{R}}_k(\boldsymbol{v}, \boldsymbol{w}, \mathbf{F}, \boldsymbol{\Theta})$ and functions therein are defined as

$$\tilde{\mathsf{R}}_k(\boldsymbol{v}, \boldsymbol{w}, \mathbf{F}, \boldsymbol{\Theta}) \triangleq \log(w_k) - w_k \mathsf{e}_k(\boldsymbol{v}, \mathbf{F}, \boldsymbol{\Theta}) + 1, \tag{16}$$

$$\mathsf{e}_k(\boldsymbol{v}, \mathbf{F}, \boldsymbol{\Theta}) \triangleq v_k^* \Upsilon_k(\mathbf{F}, \boldsymbol{\Theta}) v_k - 2\mathsf{Re}\{v_k^* \boldsymbol{h}_k^H \boldsymbol{f}_k\} + 1, \tag{17}$$

$$\Upsilon_k(\mathbf{F}, \boldsymbol{\Theta}) \triangleq \sum\nolimits_{j=1}^{K} |\boldsymbol{h}_k^H \boldsymbol{f}_j|^2 + \sigma_{\mathrm{RIS}}^2 \|\boldsymbol{\Theta}^H \boldsymbol{h}_{\mathrm{r},k}\|_2^2 + \sigma_k^2, \tag{18}$$

$\boldsymbol{w} = [w_1, \cdots, w_K]^T$ and $\boldsymbol{v} = [v_1, \cdots, v_K]^T$ are auxiliary variables introduced by WMMSE.

In the following, block coordinate descent (BCD) method will be adopted to resolve $(\mathcal{P}3)$.

1) Optimize auxiliary variable $\boldsymbol{v}$

When other variables are fixed, this subproblem can be equivalently written as $\max_{\boldsymbol{v}}(\log(w_k) - w_k \mathsf{e}_k(\boldsymbol{v}|\mathbf{F}, \boldsymbol{\Theta}))$, $k \in \mathcal{K}$, due to the absence of the objective (15). This is an unconstrained convex quadratic problem and by checking the first-order optimality condition, its optimal solution can be expressed as

$$v_k = \frac{\boldsymbol{h}_k^H \boldsymbol{f}_k}{\sum_{j=1}^{K} |\boldsymbol{h}_k^H \boldsymbol{f}_j|^2 + \sigma_{\mathrm{RIS}}^2 \|\boldsymbol{\Theta}^H \boldsymbol{h}_{\mathrm{r},k}\|_2^2 + \sigma_k^2},\ k \in \mathcal{K}. \tag{19}$$

Algorithm 1: Solving the problem $(\mathcal{P}3)$

1: Initialize $\mathbf{F}^{(0)}$, $\mathbf{\Theta}^{(0)}$ and $t=0$;
2: **repeat**
3: update $\boldsymbol{v}^{(t+1)}$ by function (19);
4: update $\boldsymbol{w}^{(t+1)}$ by function (20);
5: update $\mathbf{F}^{(t+1)}$ by solving $(\mathcal{P}4)$;
6: update $\mathbf{\Theta}^{(t+1)}$ by solving $(\mathcal{P}5)$;
7: $t:=t+1$;
8: **until** convergence

2) Optimize auxiliary variable $\boldsymbol{w}$

Similar to the procedures for updating $\boldsymbol{v}$, the optimal solution to the optimization of $\boldsymbol{w}$ can be readily obtained as

$$w_k=\mathsf{e}_k^{-1}(\boldsymbol{v},\mathbf{F},\mathbf{\Theta}),\ k\in\mathcal{K}. \tag{20}$$

3) Optimize beamforming at the AP $\mathbf{F}$

The update of $\mathbf{F}$ with the remaining variables being given reads as follows

$$(\mathcal{P}4):\ \min_{\mathbf{F}}\ \xi_{\mathrm{AP}}\sum_{k=1}^{K}\|\boldsymbol{f}_k\|_2^2+\xi_{\mathrm{RIS}}\sum_{k=1}^{K}\|\mathbf{\Theta}\mathbf{G}\boldsymbol{f}_k\|_2^2 \tag{21}$$

$$\text{s.t.}\ \sum\nolimits_{k=1}^{K}\|\boldsymbol{f}_k\|_2^2\le P_{\mathrm{AP,max}}, \tag{21a}$$

$$\xi_{\mathrm{RIS}}\left(\sum\nolimits_{k=1}^{K}\|\mathbf{\Theta}\mathbf{G}\boldsymbol{f}_k\|_2^2+\sigma_{\mathrm{RIS}}^2\|\mathbf{\Theta}\|_F^2\right)+\sum\nolimits_{m=1}^{M_{\mathrm{RIS}}}\frac{\log\left(\frac{\|\boldsymbol{\theta}_m\|_2}{\delta}+1\right)}{\log\left(\frac{1}{\delta}+1\right)}L_{\mathrm{RIS}}P_{\mathrm{c,RIS}}\le P_{\mathrm{RIS,max}}, \tag{21b}$$

$$\log(w_k)-w_k\left(v_k^*\left(\sum\nolimits_{j=1}^{K}|\boldsymbol{h}_k^H\boldsymbol{f}_j|^2+\sigma_{\mathrm{RIS}}^2\|\mathbf{\Theta}^H\boldsymbol{h}_{\mathrm{r},k}\|_2^2+\sigma_k^2\right)v_k-2\mathsf{Re}\{v_k^*\boldsymbol{h}_k^H\boldsymbol{f}_k\}+1\right)+1\ge R_k,\ k\in\mathcal{K}, \tag{21c}$$

which is a convex optimization problem and can be solved by numerical solvers, such as CVX.

4) Optimize the RIS configuration $\mathbf{\Theta}$

Here the difficulty of optimizing $\mathbf{\Theta}$ lies in the right hand side of (13) which is non-convex. To handle this issue, MM method is invoked to convexify it [16]. Specifically, we construct a convex upper-bound by linearizing it at the point of $\boldsymbol{\theta}^{(t)}$ leveraging the concavity of the logarithm function, shown as

$$\log\left(\frac{\|\boldsymbol{\theta}_m\|_2}{\delta}+1\right)\le\log\left(\frac{\|\boldsymbol{\theta}_m^{(t)}\|_2}{\delta}+1\right)+\frac{\|\boldsymbol{\theta}_m\|_2-\|\boldsymbol{\theta}_m^{(t)}\|_2}{\|\boldsymbol{\theta}_m^{(t)}\|_2+\delta},\triangleq\mathsf{g}_m\big(\boldsymbol{\theta}|\boldsymbol{\theta}^{(t)}\big),\ m\in\mathcal{M}. \tag{22}$$

Substituting (13) by (22) and after some manipulations, the subproblem w.r.t. $\boldsymbol{\theta}$ can be given by

$$(\mathcal{P}5):\ \min_{\boldsymbol{\theta}}\ \boldsymbol{\theta}^T\mathbf{P}\boldsymbol{\theta}^*+\mathsf{g}\big(\boldsymbol{\theta}|\boldsymbol{\theta}^{(t)}\big)L_{\mathrm{RIS}}P_{\mathrm{c,RIS}} \tag{23}$$

$$\text{s.t.}\ \boldsymbol{\theta}^T\mathbf{P}\boldsymbol{\theta}^*+\mathsf{g}\big(\boldsymbol{\theta}|\boldsymbol{\theta}^{(t)}\big)L_{\mathrm{RIS}}P_{\mathrm{c,RIS}}\le P_{\mathrm{RIS,max}}, \tag{23a}$$

$$\boldsymbol{\theta}^T\mathbf{Q}_k\boldsymbol{\theta}^*+2\mathsf{Re}\{\boldsymbol{q}_k^H\boldsymbol{\theta}^*\}+q_k\le r_k,\ k\in\mathcal{K}, \tag{23b}$$

$$|\theta_n|\le\beta_{n,\max},\ n\in\mathcal{N}, \tag{23c}$$

Algorithm 2: Solution to $(\mathcal{P}1)$

1: Invoke Alg. 1 to obtain $\boldsymbol{\theta}^\star$ and ranking $\{\pi_i\}_{i=1}^{M_{\mathrm{RIS}}}$;
2: Set $J_{\min}=0$ and $J_{\max}=M_{\mathrm{RIS}}$;
3: **repeat**
4: set $J=\lfloor\frac{J_{\min}+J_{\max}}{2}\rfloor$, $\mathcal{A}(J)=\{\pi_{J+1},\cdots,\pi_{M_{\mathrm{RIS}}}\}$;
5: **if** $(\mathcal{P}_{\mathcal{A}(J)})$ is feasible **then**
6: $J_{\min}=J$;
7: **else**
8: $J_{\max}=J$;
9: **end if**
10: **until** $J_{\max}-J_{\min}=1$
11: Obtain $\mathcal{A}(J_{\min})=\{\pi_{J_{\min}+1},\cdots,\pi_{M_{\mathrm{RIS}}}\}$ and perform power minimization via calling Alg. 1.

where the parameters are denoted by

$$\mathbf{H}_{\mathrm{r},k}\triangleq\mathsf{diag}(\boldsymbol{h}_{\mathrm{r},k}^H),\ \bar{\boldsymbol{q}}_{k,j}\triangleq\mathbf{H}_{\mathrm{r},k}\mathbf{G}\boldsymbol{f}_j,\ \bar{q}_{k,j}\triangleq v_k^*\boldsymbol{h}_{\mathrm{d},k}^H\boldsymbol{f}_j,$$
$$\bar{\mathbf{Q}}_{k,j}\triangleq\mathbf{H}_{\mathrm{r},k}\mathbf{G}\boldsymbol{f}_j\boldsymbol{f}_j^H\mathbf{G}^H\mathbf{H}_{\mathrm{r},k}^H,\ r_k\triangleq\log(w_k)-R_k+1,$$
$$\mathbf{P}=\xi_{\mathrm{RIS}}\left(\sum\nolimits_{k=1}^{K}\mathsf{diag}(\mathbf{G}\boldsymbol{f}_k)(\mathsf{diag}(\mathbf{G}\boldsymbol{f}_k))^H+\sigma_{\mathrm{RIS}}^2\mathbf{I}_{N_{\mathrm{RIS}}}\right),$$
$$\mathbf{Q}_k=w_k\left(\sum\nolimits_{j=1}^{K}v_k^*\bar{\mathbf{Q}}_{k,j}v_k+\sigma_{\mathrm{RIS}}^2v_k^*\mathbf{H}_{\mathrm{r},k}\mathbf{H}_{\mathrm{r},k}^Hv_k\right),$$
$$\boldsymbol{q}_k^H=w_k\left(\sum\nolimits_{j=1}^{K}\bar{q}_{k,j}\bar{\boldsymbol{q}}_{k,j}^Hv_k-\bar{\boldsymbol{q}}_{k,k}^Hv_k\right),$$
$$q_k=w_k\left(1-2\mathsf{Re}\{\bar{q}_{k,k}\}+\sum\nolimits_{j=1}^{K}|\bar{q}_{k,j}|^2+\sigma_k^2|v_k|^2\right),$$
$$\mathsf{g}\big(\phi|\phi^{(t)}\big)=\frac{\sum_{m=1}^{M_{\mathrm{RIS}}}\mathsf{g}_m\big(\phi|\phi^{(t)}\big)}{\log\left(\frac{1}{\delta}+1\right)}. \tag{24}$$

The problem $(\mathcal{P}5)$ is convex and can be numerically solved.

The overall algorithm for $(\mathcal{P}3)$ is stated in Algorithm 1.

B. Determine Activation Pattern

We proceed to determine the activation pattern of the sub-arrays based on the obtained solution $\boldsymbol{\theta}^\star$.

Observing from (22), with a small $\|\boldsymbol{\theta}_m^{(t)}\|_2,\ m\in\mathcal{M}$, the weight $1/(\|\boldsymbol{\theta}_m^{(t)}\|_2+\delta)$ will become large in the $(t+1)$th iteration to further push $\|\boldsymbol{\theta}_m\|_2$ approaching zero, which implies that the solution $\boldsymbol{\theta}^\star$ has a group sparsity structure. Intuitively, a smaller magnitude of a sub-array $\|\boldsymbol{\theta}_m^\star\|_2$ will lead to less contribution to the QoS requirements, hence, it should be switched off with a higher priority. Motivated by this fact, we can obtain a "switch-off" ranking $\{\pi_1,\cdots,\pi_{M_{\mathrm{RIS}}}\}$ such that $\|\boldsymbol{\theta}_{\pi_1}^\star\|_2\le\cdots\le\|\boldsymbol{\theta}_{\pi_{M_{\mathrm{RIS}}}}^\star\|_2$ via sorting $\|\boldsymbol{\theta}_m\|_2,\ m\in\mathcal{M}$, in an ascending manner, where π_i with a smaller i has a higher priority to be deactivated. Therefore, the active set should be $\mathcal{A}(J)=\{\pi_{J+1},\pi_{J+2},\cdots,\pi_{M_{\mathrm{RIS}}}\}$ and the maximal J is desired to be determined. In particular, bi-section search for iteratively identifying the maximal splitting point J partitioning $\mathcal{M}$ into activated and deactivated sets is adopted. For the active set $\mathcal{A}(J)$ corresponding to given J, we intend to solve a feasibility characterization problem as follows

$$(\mathcal{P}_{\mathcal{A}(J)}):\ \text{Find}\ (\mathbf{F},\mathbf{\Theta}_{m\in\mathcal{A}(\mathcal{J})}) \tag{25}$$

TABLE I: Simulation Parameters

Parameters	Values
Maximal TRP of the AP $P_{\mathrm{AP,max}}$	25dBm
Maximal power supply at the RIS $P_{\mathrm{RIS,max}}$	1W
Dissipated power of the AP $P_{\mathrm{c,AP}}$	2W
Dissipated power of each reflecting element $P_{\mathrm{c,RIS}}$	2.5mW
Dissipated power of the users $P_{\mathrm{c},k},\ k \in \mathcal{K}$	10dBm
Noise power at the RIS and users $\sigma^2_{\mathrm{RIS}}, \sigma^2_k,\ k \in \mathcal{K}$	-80dBm
Number of reflecting elements N_{RIS}	300
Amplifying coefficients $\beta_{n,\max},\ n \in \mathcal{N}$	80
Inverse of the emission efficiency of the AP ξ_{AP}	1.2
Inverse of the emission efficiency of the RIS ξ_{RIS}	1.2

$$\text{s.t.} \sum\nolimits_{k=1}^{K} \|\boldsymbol{f}_k\|_2^2 \le P_{\mathrm{AP,max}}, \tag{25a}$$

$$\mathsf{P}_{\mathrm{RIS}}(\mathbf{F}, \boldsymbol{\Theta}_{m\in\mathcal{A}(\mathcal{J})}) \le P_{\mathrm{RIS,max}}, \tag{25b}$$

$$\log(1+\mathsf{SINR}_k(\mathbf{F}, \boldsymbol{\Theta}_{m\in\mathcal{A}(\mathcal{J})})) \ge R_k,\ k \in \mathcal{K}, \tag{25c}$$

$$\beta_n \le \beta_{n,\max},\ \theta_n \in [0, 2\pi),\ n \in \mathcal{N}. \tag{25d}$$

If $(\mathcal{P}_{\mathcal{A}(J)})$ is feasible, then, we can turn off more sub-arrays in the next iteration. Otherwise, more sub-arrays should be activated to achieve QoS thresholds. Once the activation pattern is decided, the ℓ_0-norm in $(\mathcal{P}1)$ boils down to a constant. Therefore, we can invoke Alg. 1 again to attack a conventional optimization—joint beamforming design of the AP and the activated sub-arrays.

The overall procedure to handle $(\mathcal{P}1)$ is summarized in Algorithm 2.

IV. Simulation Results

In this section, we present numerical results to demonstrate the effectiveness of our proposed algorithms and the benefit of our proposed sub-array based RIS activation scheme. Consider a system where an AP equipped with $M_{\mathrm{AP}} = 8$ antennas located at the origin serves $K = 5$ users that are randomly distributed within a circle with its center at $(120\mathrm{m}, 0, 0)$ and radius of 8m with the assistance of an active RIS positioned at $(100\mathrm{m}, 0, 5\mathrm{m})$. Unless otherwise specified, the system parameters are given in Table I.

The convergence behaviour of Alg. 1 is illustrated in Fig. 3, whose left part demonstrates the convergence of solving $(\mathcal{P}3)$ and right part shows the convergence with the finally determined activation pattern. Obviously, our proposed algorithm can exhibit monotonically decreasing and fast convergence.

We investigate the impact of QoS requirements on power consumption of the system in Fig. 4. Besides our proposed algorithm, other sub-array activation schemes are also presented for comparison, which include: i) All-On: always switch on all the sub-arrays, ii) Rand.-Sel.: randomly selected 150 sub-array activation patterns for power minimization and calculate the average power, iii) Passive-RIS: replace the active RIS by a passive one with N_{RIS} elements, whose system settings are partially changed as $P_{\mathrm{c,RIS}} := 24\%P_{\mathrm{c,RIS}}$ [9] and $P_{\mathrm{AP,max}} := P_{\mathrm{AP,max}} + P_{\mathrm{RIS,max}} - N_{\mathrm{RIS}}P_{\mathrm{c,RIS}}$ for fairness, iv) No-RIS: remove the active RIS and set $P_{\mathrm{AP,max}} := P_{\mathrm{AP,max}} + P_{\mathrm{RIS,max}}$ for a fair comparison, v) Exhaust.: optimize power among all the subsets $\mathcal{A}$ and select the optima. Observed from Fig. 4, substantial power saving can be achieved by our sub-array based configuration compared to the traditional "All-On"

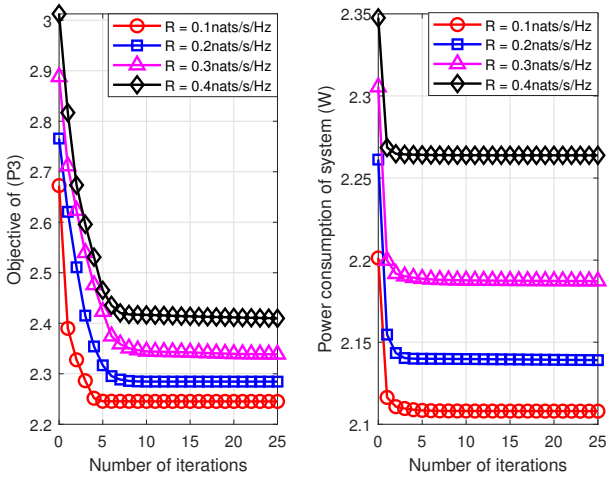

Fig. 3. Convergence of Alg. 1 and power minimization with obtained activation pattern ($M_{\mathrm{RIS}} = 15$).

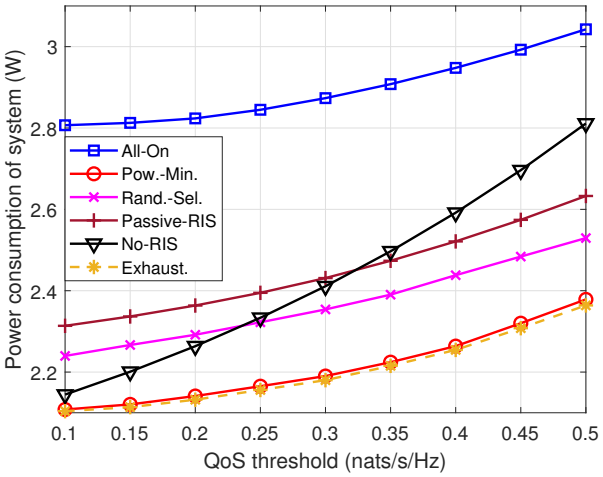

Fig. 4. The impact of QoS threshold on power consumption of the system ($M_{\mathrm{RIS}} = 15$).

scheme. Most importantly, our algorithm can well compete the performance of that obtained from the "Exhaust." case, but with a significantly lower complexity. It is worth noting that, "Passive-RIS" with $R_k \in [0.1, 0.3],\ k \in \mathcal{K}$, and "All-On" schemes yield a larger total power consumption than the "No-RIS" case, however, it should be stressed that, this phenomenon does not contradict the results from the existing literature [3], [9], since the non-transmit power of the RIS, which is usually ignored in other works considering the power minimization, is taken into account in this paper.

The impact of the granularity of the sub-arrays on the power saving performance is plotted in Fig. 5. In this experiment, N_{RIS} is still fixed at 300 while the size of sub-array L_{RIS} is varied and we examine its performance. As suggested in Fig. 5, when L_{RIS} is smaller, we can obtain more power saving gain. Intuitively, more precise activation can be accomplished via

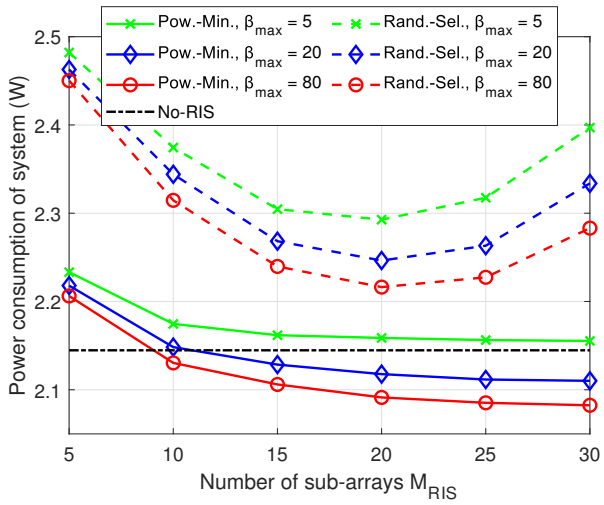

Fig. 5. The impact of number of sub-arrays on power consumption of the system ($R_k = 0.1$nats/s/Hz, $k \in \mathcal{K}$).

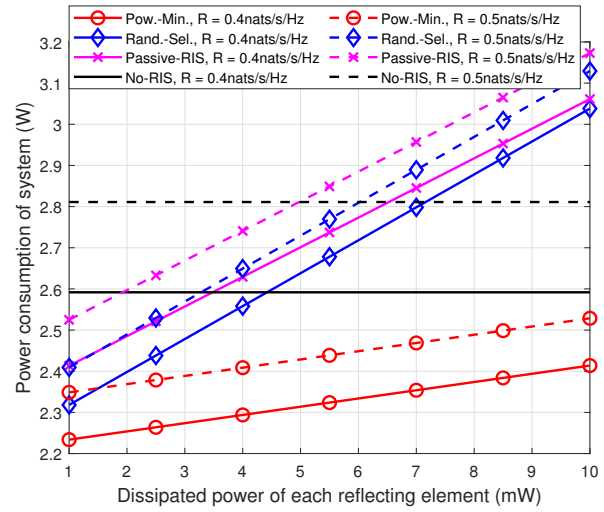

Fig. 6. The impact of non-transmit power of each active RIS element on power consumption of the system ($M_{\mathrm{RIS}} = 15$).

smaller sub-arrays, but at an expense of a higher computational complexity. Furthermore, larger amplifying coefficients can also result in power decreasing. Note that we always choose 150 random activation patterns for "Rand.-Sel." scheme. Hence, with a larger M_{RIS}, only a small fraction of the whole pattern space can be covered by these randomly selected activation patterns, which leads to performance degradation of "Rand.-Sel." case.

Fig. 6 illustrates the impact of non-transmit power expenditure of each reflecting element on system's power consumption. The system settings of "Passive-RIS" and "No-RIS" schemes are the same as those utilized in the experiment for Fig. 4. It can be seen from Fig. 6 that even when the non-transmit power of reflecting element goes up to 10mW, our proposed joint activation and beamforming scheme can achieve the best power performance among considered scenarios, while "Passive-RIS" and "Rand.-Sel." schemes are even worse than "No-RIS" case due to the substantial power consumed by the amplifiers and phase shifters.

V. Conclusion

In this paper, we design a sub-array based structure for the active RIS to reduce the non-negligible power consumption from the active reflecting elements. An efficient algorithm has been developed to tackle the power minimization problem via jointly optimizing the beamforming at the AP and the configuration of the RIS. Numerical results verify the effectiveness of our proposed solutions that can nearly coincide that obtained from the exhaustive searching method and the novel structure for remarkable power reduction.

References

[1] C. Pan and *et al.*, "Reconfigurable intelligent surfaces for 6G systems: Principles, applications, and research directions," *IEEE Commun. Mag.*, vol. 59, no. 6, pp. 14–20, Jun. 2021.

[2] Q. Wu, X. Guan, and R. Zhang, "Intelligent reflecting surface-aided wireless energy and information transmission: An overview," *Proceedings of the IEEE*, vol. 110, no. 1, pp. 150–170, Jan. 2022.

[3] Q. Wu and R. Zhang, "Beamforming optimization for wireless network aided by intelligent reflecting surface with discrete phase shifts," *IEEE Trans. Commun.*, vol. 68, no. 3, pp. 1838–1851, Mar. 2020.

[4] C. Pan, H. Ren, K. Wang, W. Xu, M. Elkashlan, A. Nallanathan, and L. Hanzo, "Multicell MIMO communications relying on intelligent reflecting surfaces," *IEEE Trans. Wireless Commun.*, vol. 19, no. 8, pp. 5218–5233, Aug. 2020.

[5] C. Huang, A. Zappone, G. C. Alexandropoulos, M. Debbah, and C. Yuen, "Reconfigurable intelligent surfaces for energy efficiency in wireless communication," *IEEE Trans. Wireless Commun.*, vol. 18, no. 8, pp. 4157–4170, Aug. 2019.

[6] E. Björnson, Ö. Özdogan, and E. G. Larsson, "Intelligent reflecting surface versus decode-and-forward: How large surfaces are needed to beat relaying?" *IEEE Wireless Commun. Lett.*, vol. 9, no. 2, pp. 244–248, Feb. 2020.

[7] Z. Zhang, L. Dai, X. Chen, C. Liu, F. Yang, R. Schober, and H. V. Poor, "Active RIS vs. passive RIS: Which will prevail in 6G?" Jan. 2022. [Online]. Available: https://arxiv.org/abs/2103.15154v4

[8] C. You and R. Zhang, "Wireless communication aided by intelligent reflecting surface: Active or passive?" *IEEE Wireless Commun. Lett.*, vol. 10, no. 12, pp. 2659–2663, Dec. 2021.

[9] R. Long, Y.-C. Liang, Y. Pei, and E. G. Larsson, "Active reconfigurable intelligent surface-aided wireless communications," *IEEE Trans. Wireless Commun.*, vol. 20, no. 8, pp. 4962–4975, Aug. 2021.

[10] L. Dong, H.-M. Wang, and J. Bai, "Active reconfigurable intelligent surface aided secure transmission," *IEEE Trans. Veh. Technol.*, vol. 71, no. 2, pp. 2181–2186, Feb. 2022.

[11] P. Zeng, D. Qiao, Q. Wu, and Y. Wu, "Throughput maximization for active intelligent reflecting surface aided wireless powered communications," *IEEE Wireless Commun. Lett.*, to appear.

[12] M. Merluzzi, N. D. Pietro, P. D. Lorenzo, E. C. Strinati, and S. Barbarossa, "Discontinuous computation offloading for energy-efficient mobile edge computing," *IEEE Trans. Green Commun. Netw.*, to appear.

[13] K. Liu, Z. Zhang, L. Dai, S. Xu, and F. Yang, "Active reconfigurable intelligent surface: Fully-connected or sub-connected?" *IEEE Commun. Lett.*, vol. 26, no. 1, pp. 167–171, Jan. 2022.

[14] Huawei AP1050DN-S access point datasheet, Huawei. [Online]. Available: https://e.huawei.com/en/material/networking/wlan/2b4fd557e436423e99059250ccaa9281, 2017.

[15] M. Tao, E. Chen, H. Zhou, and W. Yu, "Content-centric sparse multicast beamforming for cache-enabled cloud RAN," *IEEE Trans. Wireless Commun.*, vol. 15, no. 9, pp. 6118–6131, Sep. 2016.

[16] Y. Sun, P. Babu, and D. P. Palomar, "Majorization-minimization algorithms in signal processing, communications, and machine learning," *IEEE Trans. Signal Process.*, vol. 65, no. 3, pp. 794–816, Feb. 2017.

[17] Q. Shi, M. Razaviyayn, Z.-Q. Luo, and C. He, "An iteratively weighted MMSE approach to distributed sum-utility maximization for a MIMO interfering broadcast channel," *IEEE Trans. Signal Process.*, vol. 59, no. 9, pp. 4331–4340, Sep. 2011.